JOC Article

Contracted and Expanded *meso*-Alkynyl Porphyrinoids: from Triphyrin to Hexaphyrin

Alexander Krivokapic, Andrew R. Cowley, and Harry L. Anderson*

University of Oxford, Department of Chemistry, South Parks Road, Oxford OX1 3QY, UK

harry.anderson@chemistry.ox.ac.uk

Received November 21, 2002

The boron trifluoride-catalyzed Rothemund condensation of triisopropylsilyl (TIPS) propynal **1** with 3,4-diethylpyrrole in dichloromethane, followed by oxidation with 2,3-dichloro-5,6-dicyano-1,4-benzoquinone (DDQ) generates a mixture of products, including [15]triphyrin(1.1.3) H**3**, corrole H_3**4**, porphyrin H_2**2**, [24]pentaphyrin(1.1.1.1.1) H_4**5**, [28]hexaphyrin(1.1.1.1.1.1) H_4**6**, and two linear tripyrromethenes H_2**7** and H_2**8**. We report the spectroscopic characteristics of these unusual chromophores, together with the crystal structures of triphyrin H**3** (and its zinc complex ZnCl**3**), porphyrin H_2**2** (and its metal complexes Zn**2**, Ni**2** and Pt**2**), hexaphyrin H_4**6**, and tripyrromethene nickel(II) complex Ni**7**. When the condensation is catalyzed with trifluoroacetic acid, rather than boron trifluoride, the triphyrin H**3** become the main product (26% yield). This novel macrocycle is linked with a TIPS-substituted exocyclic double bond. This C═C bond makes an η^2-interaction with the zinc center in ZnCl**3** with C−Zn distances of 2.863 and 3.025 Å. The porphyrin H_2**2** is severely ruffled, and its absorption spectrum is red-shifted and broadened compared with the analogous compound without ethyl substituents. The hexaphyrin H_4**6** adopts a figure-of-eight conformation with virtual C_2 symmetry in the solid state and C_2 symmetry in solution on the NMR time scale. Oxidation with DDQ appears to convert this nonaromatic [28]hexaphyrin into an aromatic [26]hexaphyrin with a strongly red-shifted absorption spectrum, but the oxidized macrocyle is too unstable to isolate.

Introduction

The rich coordination chemistry and photochemistry of porphyrins have made them the most thoroughly studied class of macrocyclic ligands. Expanded and contracted porphyrins accommodate an even wider diversity of guests and exhibit photochemistry at a broader range of wavelengths, generating a wealth of potential applications.[1] Sessler,[2] Furuta,[3] Setsune,[4] and others[5] have recently reported many spectacular additions to this family of macrocycles. Some of these porphyrin analogues are created by design, whereas others assemble serendipitously, concurrently with porphyrins, in the acid-catalyzed Rothemund condensation of aldehydes with pyrroles.[3,6] The formation of non-porphyrin macrocycles in these reactions tends to be unpredictable, although electron-deficient aldehydes, such as pentafluorobenzaldehyde, often favor generation of expanded porphyrins.

Acetylenic aldehydes normally condense cleanly with pyrrole to generate *meso*-alkynyl porphyrins, without forming other macrocycles.[7,8] For example, boron trifluoride-catalyzed reaction of triisoproylsilyl propynal **1** with pyrrole, followed by oxidation with 2,3-dichloro-5,6-dicyano-1,4-benzoquinone (DDQ), gives the expected *meso*-tetraalkynyl porphyrin in 25% yield, with no other colored products (apart from polymeric tars). However, we have discovered that when this reaction is performed with 3,4-diethylpyrrole, instead of pyrrole, a wide range

(1) (a) Sessler, J. L.; Weghorn, S. J. *Expanded, Contracted and Isomeric Porphyrins, Tetrahedron Organic Chemistry Series*; Pergamon: Oxford, 1997; Vol. 15. (b) Sessler, J. L.; Gebauer, A.; Weghorn, S. J. In *The Porphyrin Handbook*; Kadish, K. M., Smith, K. M., Guilard, R., Eds.; Academic Press: New York, 2000; Vol. 2. (c) Jasat, A.; Dolphin, D. *Chem. Rev.* **1997**, *97*, 2267−2340. (d) Lash, T. D. *Angew. Chem., Int. Ed.* **2000**, *39*, 1763−1767. (e) Sessler, J. L.; Vivian, A. E.; Seidel, D.; Burrell, A. K.; Hoehner, M.; Mody, T. D.; Gebauer, A.; Weghorn, S. J.; Lynch, V. *Coord. Chem. Rev.* **2001**, *216−217*, 411−434.

(2) (a) Seidel, D.; Lynch, V.; Sessler, J. L. *Angew. Chem., Int. Ed.* **2002**, *41*, 1422−1425. (b) Bucher, C.; Seidel, D.; Lynch, V.; Sessler, J. L. *Chem. Commun.* **2002**, 328−329. (c) Sessler, J. L.; Seidel, D.; Bucher, C.; Lynch, V. *Chem. Commun.* **2000**, 1473−1474.

(3) (a) Shin, J.-Y.; Furuta, H.; Yoza, K.; Igarashi, S.; Osuka, A. *J. Am. Chem. Soc.* **2001**, *123*, 7190−7191. (b) Shin, J.-Y.; Furuta, H.; Osuka, A. *Angew. Chem., Int. Ed.* **2001**, *40*, 619−621. (c) Furuta, H.; Maeda, H.; Osuka, A. *Chem. Commun.* **2002**, 1795−1804.

(4) (a) Setsune, J.; Katakami, Y.; Iizuna, N. *J. Am. Chem. Soc.* **1999**, *121*, 8957−8958. (b) Setsune, J.; Maeda, S. *J. Am. Chem. Soc.* **2000**, *122*, 12405−12406.

(5) (a) Anand, V. R. G.; Pushpan, S. K.; Srinivasan, A.; Narayana, S. J.; Sridevi, B.; Chandrashekar, T. K.; Roy, R.; Joshi, B. S. *Org. Lett.* **2000**, *2*, 3829−3832. (b) Wytko, J. A.; Michels, M.; Zander, L.; Lex., J.; Schmickler, H.; Vogel, E, *J. Org. Chem.* **2000**, *65*, 8709−8714.

(6) (a) Neves, M. G. P. M. S.; Martins, R. M.; Tomé, A. C.; Silvestre, A. J. D.; Silva, A. M. S.; Félix, V.; Drew, M. G. B.; Cavaleiro, J. A. S. *Chem. Commun.* **1999**, 385−386. (b) Furuta, H.; Asano, T.; Ogawa, T. *J. Am. Chem. Soc.* **1994**, *116*, 767−768. (c) Chmielewski, P. J.; Latos-Grazynski, L.; Rachlewicz, K.; Glowiak, T. *Angew, Chem. Int. Ed. Engl.* **1994**, *33*, 779−781. (d) Chmielewski, P. J.; Latos-Grazynski, L.; Rachlewicz, K. *Chem. Eur. J.* **1995**, *1*, 68−73. (e) Geier, G. R.; Lindsey, J. S. *J. Org. Chem.* **1999**, *64*, 1596−1603.

(7) Anderson, H. L. *Tetrahedron Lett.* **1992**, *33*, 1101−1103. Anderson, H. L.; Wylie, A. P.; Prout, K. *J. Chem. Soc., Perkin Trans. 1* **1998**, 1607−1611.

(8) Milgrom, L. R.; Yahioglu, G. *Tetrahedron Lett.* **1995**, *36*, 9061−9064.

10.1021/jo026748c CCC: $25.00
Published on Web 12/31/2002

SCHEME 1

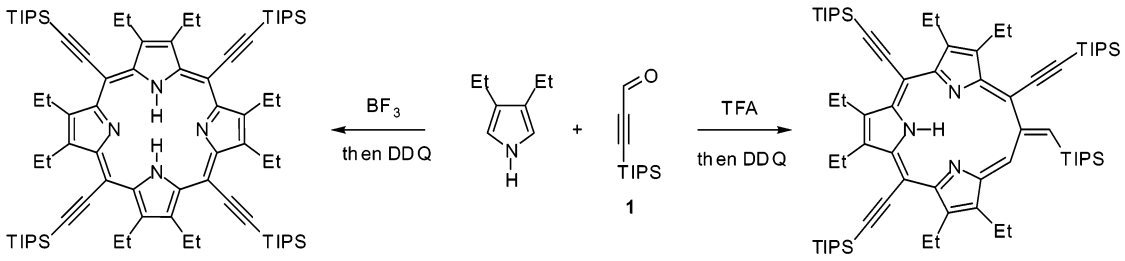

CHART 1. Structures of Byproducts from Synthesis of $H_2$2

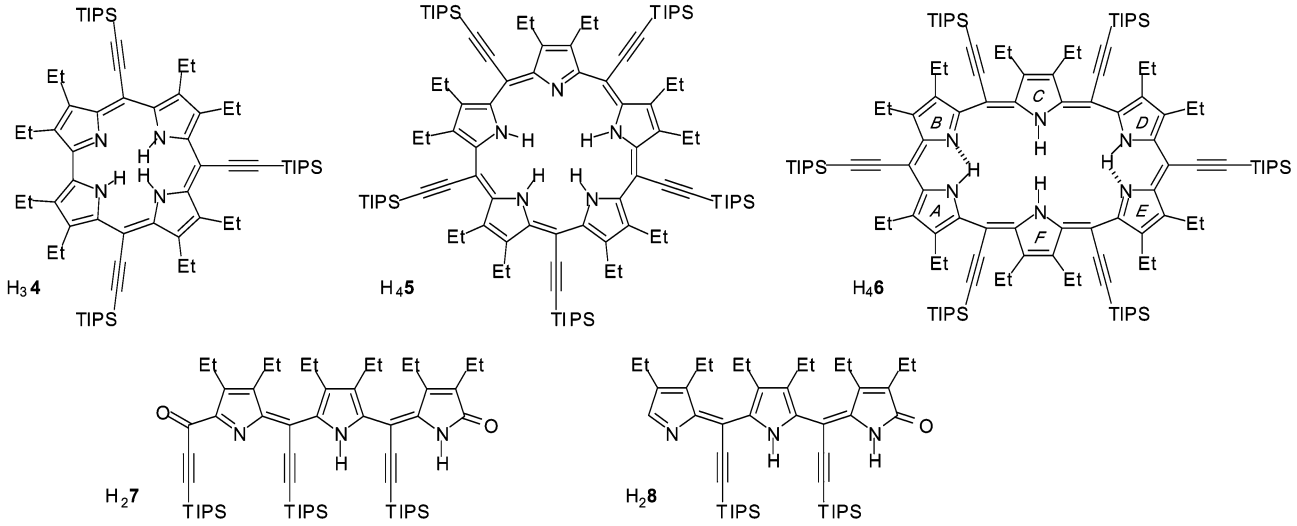

of porphyrin analogues are formed, as well as the peripherally congested porphyrin H_2**2**. The most remarkable of these byproducts is a triphyrin(1.1.3) H**3**, which is formed in 3.5% yield in the BF_3·OEt_2-catalyzed reaction and becomes the main product (26% yield) when the reaction is catalyzed with trifluoroacetic acid (Scheme 1). Other byproducts include corrole H_3**4**, pentaphyrin H_4**5**, and hexaphyrin H_4**6**, as well as two linear tripyrromethenes, H_2**7** and H_2**8** (Chart 1). Here we discuss the spectroscopic characteristics of these unusual chromophores, together with the crystal structures of triphyrin H**3** (and its zinc complex ZnCl**3**), porphyrin H_2**2** (and its metal complexes Zn**2**, Ni**2** and Pt**2**), hexaphyrin H_4**6**, and tripyrromethene nickel(II) complex Ni**7**. The crowded peripheries of these π-systems tend to make them nonplanar, and the *meso*-alkynyl substituents extend the conjugation away from the core of each chromophore, shifting the absorption to longer wavelengths.

Meso-tetraalkynyl porphyrins are promising materials for optical limiting.[9] The original aim of this work was to prepare *meso*-tetraalkynyl porphyrins with β-alkyl substituents to reduce their tendency to aggregate, since aggregation broadens the absorption, making the chromophores less effective optical limiters. To our surprise this chemistry generated a new family of contracted and expanded porphyrinoids.

Results and Discussion

Boron trifluoride-catalyzed reaction of TIPS-propynal **1** with 3,4-diethylpyrrole in dichloromethane, followed by DDQ oxidation, generates a complex mixture of colored compounds, most of which can be identified in the MALDI TOF mass spectrum of the reaction mixture (Figure 1). The mixture was separated by flash chromatography on silica to yield triphyrin H**3** (3.5%), corrole H_3**4** (6.5%), porphyrin H_2**2** (15%), pentaphyrin H_4**5** (2.4%), and hexa-

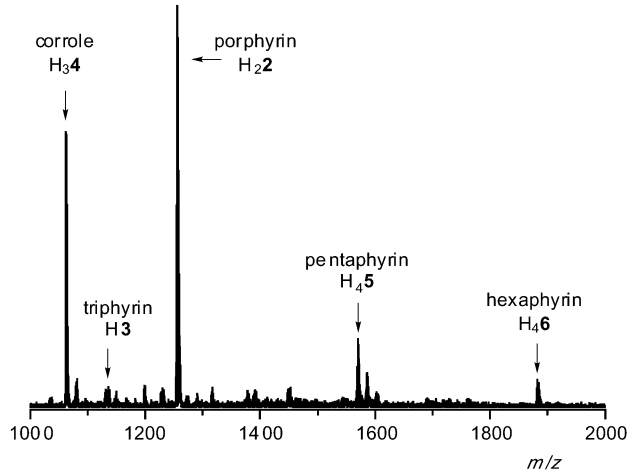

FIGURE 1. MALDI TOF mass spectrum of the crude reaction mixture from the BF_3·OEt_2-catalyzed reaction of 3,4-diethyl pyrrole and triisopropylsilyl propynal, after DDQ oxidation.

(9) Krivokapic, A.; Anderson, H. L.; Bourhill, G.; Ives, R.; Clark, S.; McEwan, K. J. *Adv. Mater.* **2001**, *13*, 652−656. McEwan, K. J.; Bourhill, G.; Robertson, J. M.; Anderson, H. L. *J. Nonlinear Opt. Phys. Mater.* **2000**, *9*, 451−468.

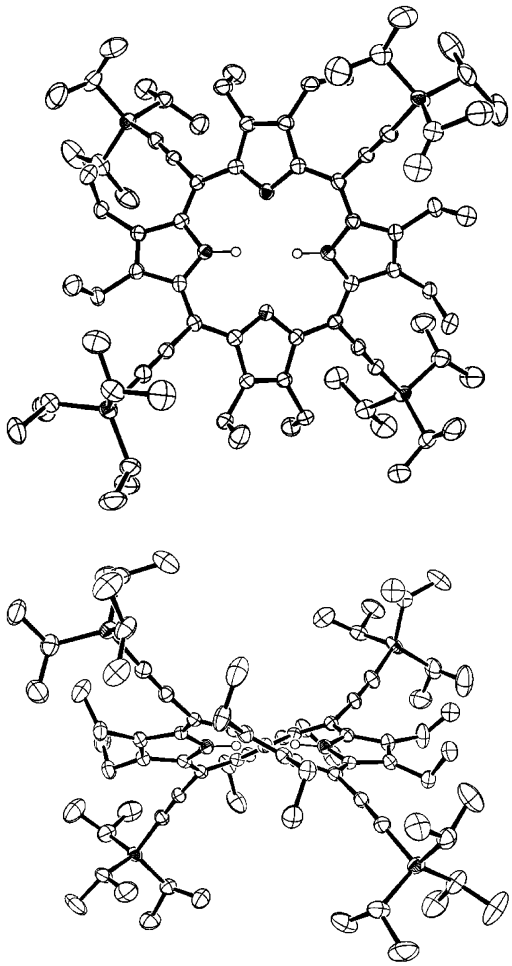

FIGURE 2. Two orthogonal views of the structure of H_2**2** in the crystal (hydrogens omitted for clarity except on nitrogen; 50% probability ellipsoids).

phyrin H_4**6** (1.4%), as well as two linear tripyrromethenes H_2**7** (7.5%) and H_2**8** (2.5%). Here we present the structural and spectroscopic characteristics of the porphyrin and then compare the other products.

Porphyrin $H_2$2. The free-base adopts a highly ruffled conformation, due to the bulk of the β-ethyl substituents, as seen from its crystal structure (Figure 2). We have also determined the crystal structures of Zn**2**, Ni**2**, and Pt**2** (see Supporting Information). The porphyrin adopts a very similar ruffled conformation in all four structures. This is seen most clearly from the overlaid radial projections in Figure 3 and shows that the conformation is locked by the peripheral substituents. The ^{1}H NMR spectrum of H_2**2** in $CDCl_3$ exhibits a NH signal at + 0.75 ppm, which is remarkably downfield for a porphyrin NH resonance; this effect seems to be characteristic of highly ruffled porphyrins and has been attributed to enhanced intramolecular hydrogen bonding.[10] The visible absorption spectra of these porphyrins are red-shifted and broadened compared with those of the analogous porphyrins without β-ethyl substituents such as H_2**9a**. For example, the Soret bands of H_2**2** and H_2**9a** peak at 498 nm (fwhm 39 nm) and 453 nm (fwhm 17 nm), respectively. The same effect is seen in the Q-band. Spectral changes of this type are often observed in highly substituted nonplanar porphyrins, and it has often been assumed that the red-shift is caused by the nonplanarity. However DiMagno has postulated that subtle in-plane distortions have a greater effect on absorption spectra.[11] Comparison of the crystallographic data shows that the C_α−C_β, C_β−C_β, and C_α−C_{meso} bond lengths in H_2**2** are longer than those in H_2**9b** by 0.020, 0.025, and 0.016 Å respectively.[12] This illustrates how crowding stretches the periphery of the π-system but does not establish whether this in-plane distortion causes the red shift.

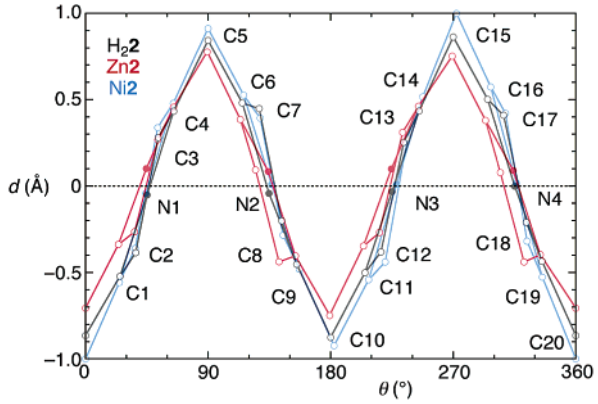

FIGURE 3. Radial projection of porphyrins H_2**2**, Zn**2**, and Ni**2** (d is the distance of each atom from the mean plane of the $C_{20}N_4$ core; θ is the angle from the centroid projected onto this plane). The projection of Pt**2**, not shown, is superimpsable with that of Zn**2**.

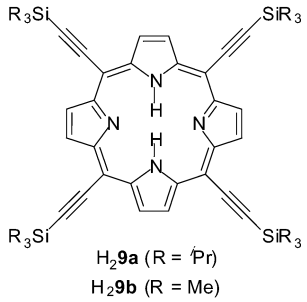

H_2**9a** (R = ^{i}Pr)
H_2**9b** (R = Me)

Triphyrin H3. The ^{1}H NMR spectrum of this bright blue product features a 1H NH singlet at 11.3 ppm, two 1H doublets at 6.88 and 5.35 ppm (J = 1.6 Hz), and a complex pattern of six diastereotopic ethyl CH_2 signals in the 3.5−2.5 ppm region. The mass spectrum gives a peak at 1136.8 Da, which is lighter than that of porphyrin H_2**2** by the mass of a diethylpyrrole unit, suggesting a tripyrrolic species. Fortunately, we were able to grow single crystals, and X-ray analysis revealed that this compound is the novel tripyrrolic macrocycle H**3**, which

(10) Somma, M. S.; Medforth, C. J.; Nelson, N. Y.; Olmstead, M. M.; Khoury, R. G.; Smith, K. M. *Chem. Commun.* **1999**, 1221−1222.

(11) Shelnutt, J. A.; Song, X.-Z.; Ma, J.-G.; Jia, S.-L.; Jentzen, W.; Medforth, C. J. *Chem. Soc. Rev.* **1998**, *27*, 31−41. Wentsching, A. K.; Koch, A. S.; DiMagno, S. G. *J. Am. Chem. Soc.* **2001**, *123*, 3932−3939. Parusel, A. B. J.; Wondimagegn, T.; Ghosh, A. *J. Am. Chem. Soc.* **2000**, *122*, 6371−6374.

(12) Da Cruz, F.; Armand, F.; Albouy, P.-A.; Nierlich, M.; Ruaudel-Teixier, A. *Langmuir* **1999**, *15*, 3653−3660. We thank the authors of this article for providing us with the crystallographic data for compound H_2**9b**.

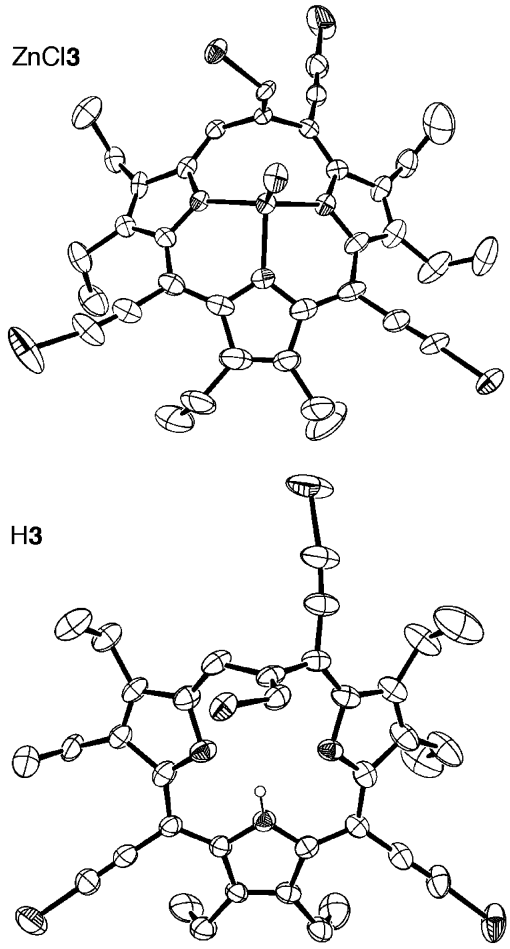

FIGURE 4. Structures of H**3** and ZnCl**3** in the solid state (hydrogens omitted, except on nitrogen, and *iso*-propyl groups omitted for clarity; 50% probability ellipsoids).

by extension of Franck's nomenclature,[13] we call a [15]-triphyrin(1.1.3).

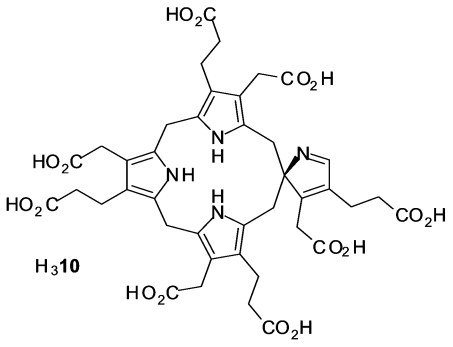

We also determined the crystal structure of zinc chloride complex ZnCl**3** (Figure 4). The only previously known macrocycles with this type of framework are compounds such as spiro-pyrrolenine H_3**10**, which is believed to be an intermediate in the biosynthesis of uroporphyrinogen III.[14] The single NH hydrogen of H**3** is located on the nitrogen of the central pyrrole unit, both from the residual electron-density map and from the wider N−C−N bond angle at this nitrogen (110.3° compared with 106.5 and 106.0° at the other two nitrogens). The bond-length alternation pattern also confirms that this tautomer is favored in the crystal. The macrocycle is linked by a TIPS-substituted exocyclic double bond, which rises up almost perpendicular to the mean plane of the three pyrrole rings. This explains why all 12 CH_2 protons are inequivalent and accounts for the observation of two alkene proton resonances with weak four-bond coupling. The exocyclic double bond is obviously formed by addition across a triple bond, probably via protonation of the alkyne to form an allene, which then cyclizes, as in Scheme 2. This mechanism implies that the triphyrin will be formed more efficiently under Brønsted acid catalysis, and indeed we found that use of trifluoroacetic acid instead of BF_3·OEt_2 increases the yield of H**3** from 3.5 to 26%. Under these conditions, triphyrin H**3** is the only macrocyclic product. The electronic absorption spectra of free-base triphyrin H**3** and porphyrin H_2**2** are compared in Figure 5. Both compounds absorb over the same wavelength range, but the triphyrin lacks any intense peak analogous to the porphyrin Soret band. The crystal structure of zinc(II) complex ZnCl**3** reveals a remarkable interaction between the exocyclic C=C bond and the zinc atom, as detailed in Figure 6. Both of the Zn···C distances (2.863 and 3.025 Å) are less than the sum of the van der Waals radii (3.17 Å),[15] and the shorter of these two distances is in the range reported for zinc η^2-alkene complexes.[16] The existence of a favorable Zn···C=C interaction is supported by the observation that the ZnCl moiety complexes to the more crowed face of the macrocycle. A similar chelation-promoted η^2-interaction was recently reported in a tetraphenyl-*p*-benziporphyrin cadmium(II) complex.[17]

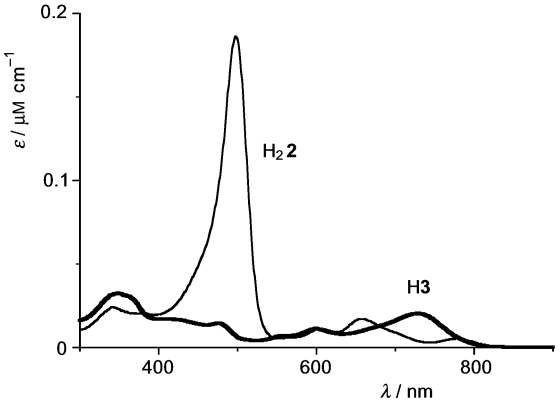

FIGURE 5. UV−visible absorption spectra of porphyrin H_2**2** (plain) and triphyrin H**3** (bold) in CH_2Cl_2.

Corrole $H_3$4 was isolated as a green band running slightly slower than the porphyrin. It was readily identified from its NMR and mass spectra. Concurrent formation of corroles during porphyrin synthesis is precedent-

(13) Gosmann, M.; Frank, B. *Angew. Chem., Int. Ed. Engl.* **1986**, *25*, 1100−1101.

(14) Mathewson, J. H.; Corwin, A. H. *J. Am. Chem. Soc.* **1961**, *83*, 135−137. Stark, W. M.; Hart, G. J.; Battersby, A. R. *J. Chem. Soc., Chem. Commun.* **1986**, 465−467. Scott, A. I. *Acc. Chem. Res.* **1990**, *23*, 308−317.

(15) Bondi, A. *J. Phys. Chem.* **1964**, *68*, 441−451.

(16) Benn, R.; Grondey, H.; Lehmkuhl, H.; Nehl, H.; Angermund, K. Krüger, C. *Angew. Chem., Int. Ed. Engl.* **1987**, *26*, 1279−1280.

(17) Stepien, M.; Latos-Grazynski, L. *J. Am. Chem. Soc.* **2002**, *124*, 3838−3839.

SCHEME 2. Proposed Mechanism of Formation of Triphyrin H3

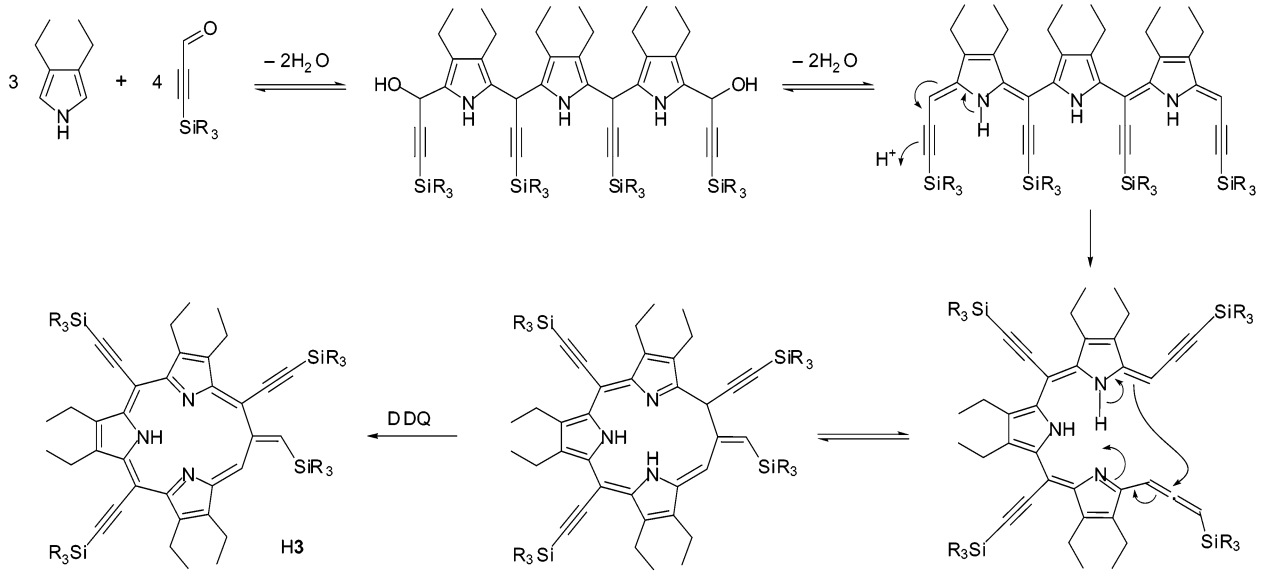

ed[18] and probably occurs during the DDQ oxidation step, by oxidative cyclization of linear tetrapyrromethanes.[19] The corrole exhibits a Soret-like absorption band at 474 nm (fwhm 49 nm); its absorption spectrum is similar to that of H_2**2** but broader and less red-shifted.

[28]Hexaphyrin(1.1.1.1.1.1) $H_4$6 was identified from its X-ray crystal structure (Figure 7).[20] Hexaphyrins were first synthesized by Gossauer,[21] who prepared the β-alkyl *meso*-unsubstituted macrocycles. *meso*-Aryl hexaphyrin-(1.1.1.1.1.1)s have also been reported[3a,6a,22] and characterized by X-ray crystallography,[6a] but these macrocycles have not previously been reported with both *meso*- and β-substituents. H_4**6** is far from planar, and the π-system adopts a "figure-of-eight" conformation in the solid-state reminiscent of larger expanded porphyrins.[2a,3a,4,23] The two central pyrrole rings (*C* and *F* in Chart 1 and Figure 7) overlap in an almost parallel offset geometry with a plane-to-plane distance of about 3.9 Å. The structure features two planar dipyrromethene wings (pyrroles *A* + *B* and *D* + *E*), each of which is held flat by hydrogen-bonding (deviation from mean plane < ±0.09 Å). The NH protons were directly identified from the residual electron-density map, and their locations on pyrroles *A*, *C*, *D*, and *F* are supported by the wider C−N−C bond angles at these nitrogens (109.9, 112.0, 110.3, and 111.9°, respectively, compared to 107.6 and 107.9° at rings *B* and *E*, respectively) as well as by the pattern of bond-length alternation. The presence of four NH protons is confirmed from integration of the ^{1}H NMR spectrum and from the mass spectrum. In the solid state, H_4**6** has virtual C_2 symmetry, and the solution ^{1}H and ^{13}C NMR spectra are also consistent with C_2 symmetry. Thus, there are two 2H NH singlets (at 15.8 and 11.7 ppm), six nonequivalent ethyl environments, each with diastereotopic methylenes, and three nonequivalent TIPS environments. This hexaphyrin has a ring of 28 π-electrons and thus is not expected to be aromatic, and the chemical shifts of the

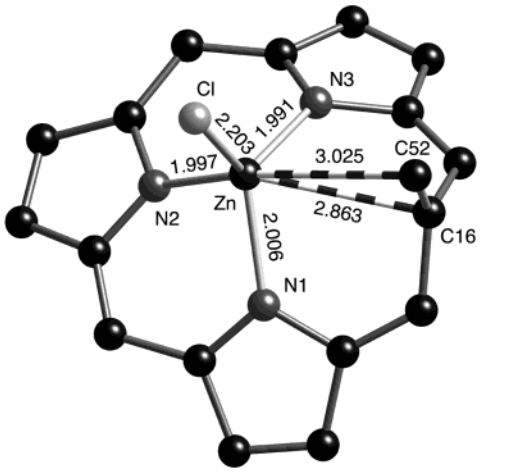

FIGURE 6. Detail of the solid-state structure of ZnCl**3** showing the coordination geometry.

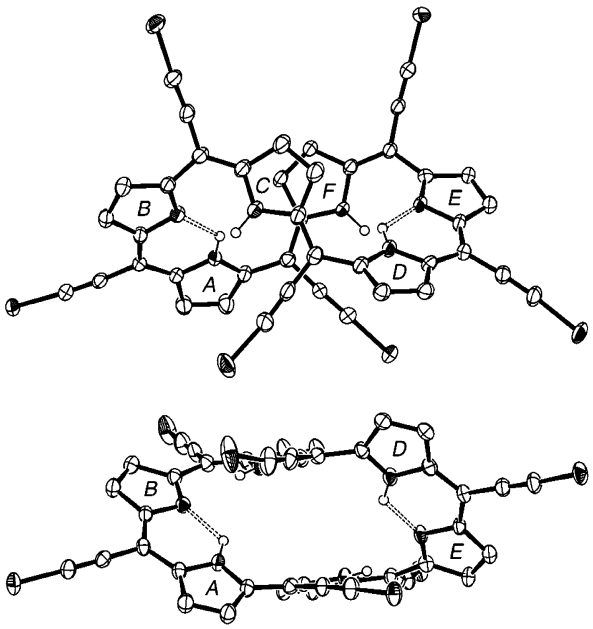

FIGURE 7. Two orthogonal views of the structure of H_4**6** in the H_4**6**·CH_2Cl_2·$2H_2O$ crystal (hydrogens omitted, except on nitrogen, and *i*-Pr and Et groups omitted for clarity; 50% probability ellipsoids).

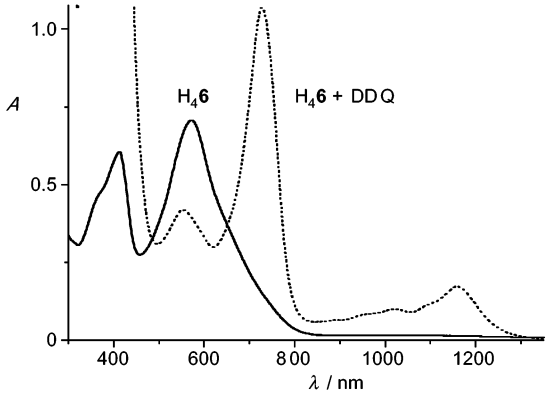

FIGURE 8. Absorption spectra of H_4**6** (1.2×10^{-5} M) in CH_2Cl_2 before (plain) and after (dotted) addition of excess solid DDQ.

NH resonances show that it has no ring current. Addition of DDQ to a solution of H_4**6** results in a dramatic sharpening and red-shifting in the UV−visible−NIR absorption bands, as illustrated in Figure 8, which suggests that the macrocycle can be oxidized to the aromatic [26]hexaphyrin(1.1.1.1.1.1);[3a,6a] however, all attempts at isolation of this oxidized hexaphyrin resulted in decomposition and reformation of H_4**6**; probably the macrocycle is too crowed to adopt a stable delocalized aromatic structure.[24]

Pentaphyrin $H_4$5 was identified from its mass spectrum. Although this macrocycle appears to be formed more efficiently than the hexaphyrin (from isolated yields and from the MALDI spectrum in Figure 1), it is rather unstable, which hindered its purification and characterization. Similar instability has been reported with *meso*-aryl pentaphyrins,[3b,25] and most known pentaphyrin(1.1.1.1.1)s are *meso*-unsubstituted. The observation of

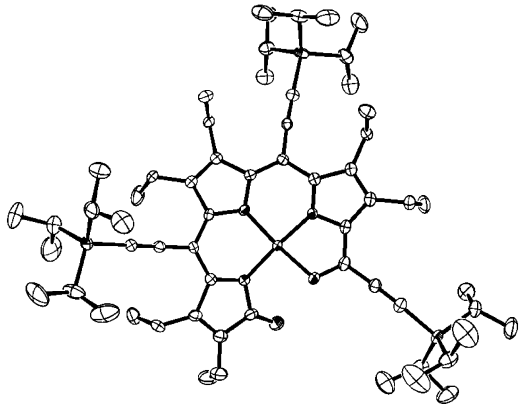

FIGURE 9. Structure of Ni**7** in the crystal (hydrogens omitted for clarity; 50% probability ellipsoids)

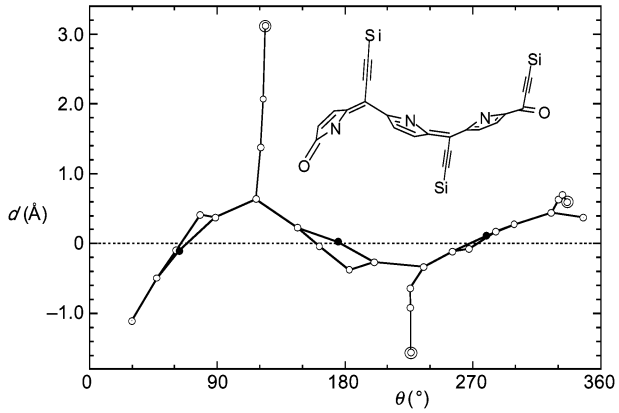

FIGURE 10. Radial projection of Ni**7** (*d* is the distance of each atom from the mean plane of the $C_{20}N_4$ core; θ is the angle from the centroid projected onto this plane).

NH peaks in the ^{1}H NMR spectrum at 10.41, 7.85, and 5.71 ppm shows that it has no ring current, and the molecular weight from FAB-MS indicates that it is a nonaromatic [24]pentaphyrin H_4**5** rather than an aromatic [22]pentaphyrin H_2**5**.

Tripyrromethenes $H_2$7 and $H_2$8 were identified from their NMR and mass spectra. Both these compounds appear to be formed by oxidation of linear tripyrrolic intermediates. H_2**7** forms stable complexes with copper(II), nickel(II), and palladium(II), and we succeeded in determining the crystal structure of the nickel(II) complex (Figure 9). The π-system of this complex is fairly planar, although it exhibits a slight helical twist due to the steric clash between the two carbonyl oxygens, as seen from the radial projection in Figure 10. The O···O distance (2.743 Å) is 0.42 Å less than twice the van der Waals radius of oxygen. Similar tripyrrolic palladium(II) and copper(II) complexes have been reported.[26,27] The UV−visible absorption spectra of H_2**7** and Ni**7** are compared in Figure 11. Formation of the nickel complex makes the absorption sharper and more red-shifted, probably by locking the conformation of the π-system. Some closely related complexes M**11** (M = Zn, Cu, Ni,

(18) Rose, E.; Kossanyi, A.; Quelquejeu, M.; Soleilhavoup, M.; Duwavran, F.; Bernard, N.; Lecas, A. *J. Am. Chem. Soc.* **1996**, *118*, 1567−1568. Gross, Z.; Galili, N.; Saltsman, I. *Angew. Chem., Int. Ed.* **1999**, *38*, 1427−1429. Spence, J. D.; Lash, T. D. *J. Org. Chem.* **2000**, *65*, 1530−1539. Paolesse, R.; Nardis, S.; Sagone, F.; Khoury, R. G. *J. Org. Chem.* **2001**, *66*, 550−556. Gryko, D. T.; Jadach, K. *J. Org. Chem.* **2001**, *66*, 4267−4275.

(19) Ka, J.-W.; Cho, W.-S.; Lee, C.-H. *Tetrahedron Lett.* **2000**, *41*, 8121−8125. Briñas, R. P.; Brückner, C. *Synlett* **2001**, 442−444. Asokan, C. V.; Smeets, S.; Dehaen, W. *Tetrahedron Lett.* **2001**, *42*, 4483−4485.

(20) Crystal structure of H_4**6** discussed here is that of the dichloromethane solvate. We have also determined the crystal structure of the toluene solvate of this compound (see Supporting Information); the molecular structure of H_4**6** in these two crystals is essentially identical.

(21) (a) Gossauer, A. *Bull. Soc. Chim. Belg.* **1983**, *92*, 793−795. (b) Charrière, R.; Jenny, T. A.; Rexhausen, H.; Gossauer, A. *Heterocycles* **1993**, *36*, 1561−1575.

(22) Brückner, C.; Sternberg, E. D.; Boyle, R. W.; Dolphin, D. *Chem. Commun.* **1997**, 1689−1690.

(23) (a) Sessler, J. L.; Weghorn, S. J.; Lynch, V.; Johnson, M. R. *Angew. Chem., Int. Ed. Engl.* **1994**, *33*, 1509−1512. (b) Vogel, E.; Bröring, M.; Fink, J.; Rosen, D.; Schmickler, H.; Lex, J.; Chan, K. W. K.; Wu, Y.-D.; Plattner, D. A.; Nendel, M.; Houk, K. N. *Angew. Chem., Int. Ed. Engl.* **1995**, *34*, 2511−2514. (c) Bröring, M.; Jendryn, J.; Zander, L.; Schmickler, H.; Lex, J.; Wu, Y.-D.; Nendel, M.; Chen, J.; Plattner, D. A.; Houk, K. N.; Vogel, E. *Angew. Chem., Int. Ed. Engl.* **1995**, *34*, 2515−2517.

(24) Cyclic voltammetry of H_4**6** in CH_2Cl_2 containing 0.5 mM Bu_4BF_4 with a Pt working electrode shows that this hexaphyrin is very easily oxidized; it displays reversible oxidation waves at −0.405, 0.060, and 0.855 V relative to internal ferrocene, whereas the first oxidation of H_2**2** occurs at 0.145 V.

(25) Rexhausen, H.; Gossauer, A. *J. Chem. Soc., Chem. Commun.* **1983**, 275. Danso-Danquah, R. E.; Xie, L. Y.; Dolphin, D. *Heterocycles* **1995**, *41*, 2553−2564. Burrell, A. K.; Hemmi, G.; Lynch, V.; Sessler, J. L. *J. Am. Chem. Soc.* **1991**, *113*, 4690−4692.

(26) Bröring, M.; Brandt, C. D. *Chem. Commun.* **2001**, 499−500. Sessler, J. L.; Gebauer, A.; Král, V.; Lynch, V. *Inorg. Chem.* **1996**, *35*, 6636−6637.

(27) Furuta, H.; Maeda, H.; Osuka, A. *Org. Lett.* **2002**, *4*, 181−184.

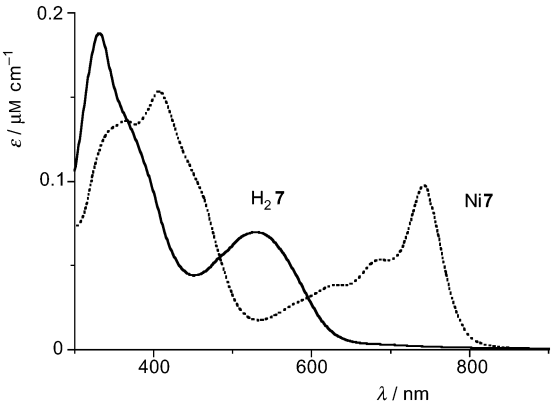

FIGURE 11. Absorption spectra of H_2**7** (plain) and Ni**7** (dotted) in CH_2Cl_2.

Pd, Pt) have been reported recently by Furuta et al.[27] and show similar structural and spectroscopic features, although the main absorption band of Ni**7** is red shifted by 100 nm relative to that of Ni**11** due to the extra conjugation with the acetylenic substituents.

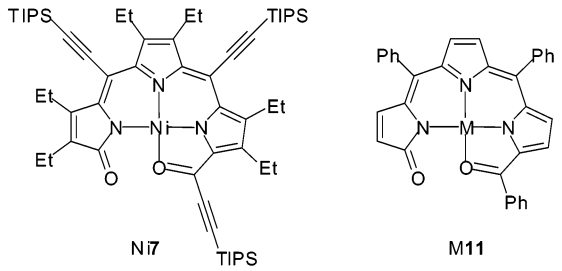

Conclusions

This work illustrates how β-alkyl substituents can control the course of a Rothemund condensation, hindering the formation of porphyrin and leading to the isolation of porphyrin analogues. In this case the β-ethyl groups probably also facilitate the isolation of porphyrin analogues by increasing their kinetic stability. For example, the TFA-catalyzed reaction of pyrrole with triisopropylsilyl propynal does not give triphyrin or porphyrin; probably the unsubstituted triphyrin is formed and reacts further to give a complex mixture of products. Triphyrin ligand H**3** has a remarkable $N_3(\eta^2$-C=C) donor set and is likely to form organometallic complexes with many metals that would not normally form η^2-alkene complexes. The figure-of-eight conformation of the hexaphyrin H_4**6** is different from that of previously reported hexaphyrins and resembles that of higher porphyrin analogues. None of these contracted and expanded porphyrinoids are formed when pyrrole is used instead of 3,4-diethyl pyrrole.

Experimental Section

General. FAB mass spectra were obtained from 3-nitrobenzyl alcohol matrix. MALDI-TOF mass spectra were recorded from anthracene-1,8,9-triol matrix; only molecular ions are reported. 3,4-Diethyl-pyrrole[28] and triisopropylsilylpropynal[29] **1** were synthesized according to published procedures.

Boron Trifluoride-Catalyzed Reaction of 3,4-Diethyl Pyrrole and Triisopropylsilylpropynal. BF_3·OEt_2 (122 μL) was added to a solution of 3,4-diethylpyrrole (1.01 mL, 7.47 mmol) and triisopropylsilylpropynal **1** (1.1 mL, 7.5 mmol) in CH_2Cl_2 (170 mL) under nitrogen. After 2 h, DDQ (1.7 g, 7.5 mmol) was added followed by triethylamine (1.5 mL). After stirring for 30 min, the reaction mixture was purified by chromatography (silica, CH_2Cl_2) with gradient addition of diethyl ether up to 1:1. The last fractions after the porphyrin were rechromatographed (silica, 60−80 petroleum ether/toluene (19:1)) with gradient addition of toluene. The following products were isolated.

[28]Hexaphyrin(1.1.1.1.1.1) $H_4$6. Yield: 32 mg, 1.4%. UV/vis (CH_2Cl_2) λ_{max}, nm (log ϵ): 260 (4.51), 415 (4.72), 572 (4.76). ^{1}H NMR (500 MHz, $CDCl_3$): δ 15.82 (2H, s), 11.71 (2H, s), 3.41−3.37 (2H, m), 3.22−3.18 (2H, m), 3.14−3.10 (2H, m), 3.00−2.89 (4H, m), 2.84−2.74 (6H, m), 2.62−2.56 (4H, m), 2.49−2.43 (4H, m), 1.51 (6H, t, J = 7.5 Hz), 1.24−1.10 (126H, m), 1.07 (6H, t, J = 7.5 Hz), 1.02 (6H, t, J = 7.5 Hz), 0.99 (6H, t, J = 7.5 Hz), 0.92 (6H, t, J = 7.5 Hz), 0.74 (6H, t, J = 7.5 Hz). ^{13}C NMR (62.5 MHz, $CDCl_3$): δ 159.0, 156.6, 145.5, 143.0, 142.6, 139.3, 139.0, 138.9, 138.5, 137.9, 136.8, 132.2, 110.6, 105.9, 105.8, 104.4, 101.6, 101.0, 99.2, 96.5, 89.2, 19.4, 19.3, 19.2, 19.1, 19.0, 18.5, 18.3, 17.7, 17.0, 16.9, 16.6, 15.8, 15.6, 13.7, 12.4. FAB-MS: m/z 1884.5 (M^+). Anal. Calcd for $C_{120}H_{190}N_6Si_6$: C, 76.45; H, 10.16; N, 4.46. Found: C, 76.52; H, 10.42; N, 4.50.

[24]Pentaphyrin(1.1.1.1.1) $H_4$5. Yield: 55 mg, 2.4%. UV/vis (CH_2Cl_2) λ_{max}, nm: 454, 745. ^{1}H NMR (250 MHz, $CDCl_3$): δ 10.41 (1H, br s), 7.85 (2H, s), 5.71 (1H, s), 3.20−3.05 (8H, m), 2.95−2.75 (8H, m), 2.10−1.95 (4H, m), 1.29−1.02 (129H, m), 0.67 (6H, m). ^{13}C NMR (62.9 MHz, $CDCl_3$): δ 158.1, 147.6, 147.3, 142.6, 141.5, 140.6, 128.8, 127.3, 126.2, 107.0, 105.6, 102.0, 101.5, 97.2, 89.6, 86.0, 18.7, 18.4, 17.9, 16.2, 16.0, 15.6, 13.3, 11.9, 11.7, 11.5. FAB-MS m/z: 1571.3 (M^+, $C_{100}H_{159}N_5Si_5$ requires 1571.79).

Corrole $H_3$4. Yield: 130 mg, 6.5%. UV/vis (CH_2Cl_2) λ_{max}, nm (log ϵ): 474 (5.07), 640 (4.37), sh 680 (4.3), sh 729 (4.0). ^{1}H NMR (500 MHz, $CDCl_3$): δ 4.12−4.05 (8H, m), 4.00 (4H, q, J = 7.5 Hz), 3.72 (4H, q, J = 7.5 Hz), 1.58 (6H, t, J = 7.5 Hz), 1.50−1.28 (81H, m), −0.75 (3H, s). ^{13}C NMR (125 MHz, $CDCl_3$): δ 139.2, 138.1, 138.0, 137.4, 137.1, 133.5, 132.2, 128.5, 107.3, 106.1, 105.2, 103.0, 94.0, 88.7, 20.0, 19.8, 19.5, 18.9, 17.7, 17.5, 17.4, 17.3, 12.2, 12.1. ES-HRMS: calcd for ($C_{68}H_{106}N_4Si_3$ + H^+) 1063.7805, found 1063.7798.

Porphyrin $H_2$2. Yield: 350 mg, 15%. UV/vis (CH_2Cl_2) λ_{max}, nm (log ϵ): 498 (5.27), 607 (4.05), 658 (4.23), 777 (3.69). ^{1}H NMR (200 MHz, $CDCl_3$): δ 4.01 (16H, q, J = 7.5 Hz) 1.51 (24H, t, J = 7.5 Hz), 1.43−1.34 (84H, m), 0.75 (2H, s). ^{13}C NMR (50 MHz, $CDCl_3$): δ 143.9 112.1, 105.7, 98.9, 20.0, 18.7, 17.2, 11.8. FAB-MS: m/z 1255.3 (M^+). Anal. Calcd for $C_{80}H_{126}N_4Si_4$: C, 76.49; H, 10.11; N, 4.46. Found C, 76.44; H, 10.40; N, 4.47.

[15]Triphyrin(1.1.3) H3. Yield: 100 mg, 3.5%. UV/vis (CH_2Cl_2) λ_{max}, nm (log ϵ): 338 (4.60), 624 (4.37). ^{1}H NMR (500 MHz, $CDCl_3$): δ 11.30 (1H, s), 6.88 (1H, d, J = 1.6 Hz), 5.35 (1H, d, J = 1.6 Hz), 3.45−3.40 (2H, m), 3.36−3.32 (2H, m), 3.17−3.10 (2H, m), 3.04−2.99 (2H, m), 2.71−2.66 (2H, m), 2.63−2.58 (2H, m), 1.3−0.7 (102H, m). ^{13}C NMR (125 MHz, $CDCl_3$): δ 166.7, 165.9, 156.0, 155.5, 149.7, 149.6, 147.7, 145.3, 145.1, 143.0, 142.8, 142.5, 141.7, 128.3, 121.4, 115.1, 107.9, 105.7, 105.5, 105.1, 101.5, 101.1, 94.4, 93.8, 19.5, 19.4, 19.3, 19.23, 19.19, 19.17, 19.13, 19.10, 18.3, 16.8, 16.7, 16.6, 16.5, 16.4, 16.2, 12.5, 12.4, 12.3, 12.1, 12.0. ES-HRMS: calcd for ($C_{72}H_{117}N_3Si_4$ + H^+) 1136.8403, found 1136.8405.

Tripyrrenone $H_2$7. Yield: 63 mg, 2.5%. UV/vis (CH_2Cl_2) λ_{max}, nm (log ϵ): 331 (4.57), 530 (4.14). IR (CCl_4): ν 2125, 1713 cm^{-1}. ^{1}H NMR (500 MHz, $CDCl_3$): δ 11.36 (1H, s), 9.67 (1H, s), 3.03−2.96 (8H, m), 2.84 (2H, q, J = 7.5 Hz), 2.38 (2H, q, J

(28) Sessler, J. L.; Mozaffari, A.; Johnson, M. R. *Org. Synth.* **1998**, *9*, 242−247.

(29) Screen, T. E. O.; Lawton, K. B.; Wilson, G. S.; Dolney, N.; Ispanoiu, R.; Goodson, T.; Martin, S. J.; Bradley, D. D. C.; Anderson, H. L. *J. Mater. Chem.* **2001**, *11*, 312−320.

TABLE 1. Summary of Crystal Data for H3, ZnCl3, $H_2$2, $H_4$6 (CH_2Cl_2 Solvate), and Ni7

	H**3**	ZnCl**3**	H_2**2**	H_4**6**	Ni**7**
formula	$C_{72}H_{117}N_3Si_4$	$C_{72}H_{116}N_3Si_4ZnCl$	$C_{80}H_{126}N_4Si_4 \cdot H_2O \cdot CH_2Cl_2$	$C_{120}H_{190}N_6Si_6 \cdot CH_2Cl_2 \cdot 2H_2O$	$C_{60}H_{93}N_3O_2Si_3Ni$
formula weight	1137.09	1236.92	1359.17	2006.31	1031.39
crystal system	monoclinic	orthorhombic	triclinic	triclinic	orthorhombic
space group	$P2_1/a$	*Pcab*	*P*-1	*P*-1	*Pbca*
a/Å	15.6985(2)	14.8345(2)	15.2870(7)	14.2769(2)	18.0619(2)
b/Å	17.2437(2)	30.4586(3)	15.6170(9)	17.7899(5)	22.7317(3)
c/Å	27.4997(5)	34.0301(5)	19.0320(11)	27.2490(4)	29.3777(4)
α/deg	90	90	107.214(3)	73.7478(5)	90
β/deg	92.4291(5)	90	106.306(3)	74.9380(5)	90
γ/deg	90	90	92.789(3)	71.4691(5)	90
V/Å^3	7437.5(2)	15376.1(3)	4122.3(4)	6187.7(2)	12061.8(3)
Z	4	8	2	2	8
T/K	150	150	150	150	150
crystal size, mm^3	0.10 × 0.05 × 0.05	0.40 × 0.14 × 0.08	0.50 × 0.40 × 0.30	0.20 × 0.16 × 0.12	0.10 × 0.09 × 0.05
reflections measured	11 681	26 428	51 968	49 636	24 074
unique reflections	11 285	14 465	15 598	27 876	12 224
R_1	0.1480	0.1203	0.0919	0.0763	0.0451
wR_2	0.1045	0.1178	0.0897	0.0915	0.0476

= 7.5 Hz), 1.27−1.06 (81H, m). ^{13}C NMR (125 MHz, $CDCl_3$): *δ* 169.9, 167.8, 165.0, 155.1, 147.8, 147.6, 146.3, 142.5, 137.6, 135.1, 133.5, 131.5, 131.2, 116.6, 109.1, 104.2, 102.8, 102.1, 100.6, 97.4, 95.5, 19.2, 19.0, 18.6, 18.5, 18.1, 17.5, 16.82, 16.79, 16.2, 15.9, 15.18, 15.16, 13.7, 11.6, 11.5, 11.1. FAB-HRMS: calcd for ($C_{60}H_{95}N_3O_2Si_3 + H^+$) 974.6810, found 974.6843.

Tripyrrenone $H_2$8. Yield: 150 mg, 7.8%. UV/vis (CH_2Cl_2) λ_{max}, nm (log ϵ): 376 (4.47), 555 (4.35). IR (KBr): 2122, 1708, 1691 cm^{-1}. ^{1}H NMR (500 MHz, $CDCl_3$): *δ* 6.91, (1H, s), 3.13−2.99 (6H, m), 2.76 (2H, q, 7.5), 2.44 (2H, q, 7.5), 2.41 (2H, q, 7.5), 1.26−1.05 (60H, m). ^{13}C NMR (125 MHz, $CDCl_3$): *δ* 170.2, 160.7, 148.5, 147.5, 146.2, 144.8, 138.1, 137.0, 136.9, 129.2, 128.7, 126.3, 119.6, 107.2, 102.9, 102.5, 100.9, 99.6, 19.4, 19.1, 18.7, 18.6, 18.5, 17.9, 17.8, 16.8, 16.6, 16.5, 15.5, 15.3, 14.5, 13.9, 11.9, 11.6. FAB-MS *m*/*z*: 767.1 (MH^+). Anal. Calcd for $C_{48}H_{75}N_3OSi_2$: C, 75.23; H, 9.87; N, 5.48. Found: C, 74.71; H, 10.37; N, 5.32.

Trifluoroacetic Acid-Catalyzed Reaction of 3,4-Diethylpyrrole and Triisopropylsilylpropynal. TFA (153 μL, 2.0 mmol) was added to a solution of 3,4-diethylpyrrole (135 μL, 1.0 mmol) and triisopropylsilylpropynal **1** (260 μL, 1.1 mmol) in CH_2Cl_2 (50 mL) under nitrogen. After 20 min, DDQ (0.18 g, 0.8 mmol) and triethylamine (2.23 mL) were added. After stirring for 30 min, the reaction mixture was purified by chromatography (silica/CH_2Cl_2) with gradient addition of diethyl ether. Triphyrin H**3** was obtained as dark blue crystals (80 mg, 26%). No porphyrin or other colored products were formed in this reaction.

X-ray Analysis. Crystals of H**3**, ZnCl**3**, H_2**2**, and H_4**6** were grown from dichloromethane by layered addition of methanol. Crystals of Ni**7** were grown from toluene by layered addition of methanol. Crystal data for H**3**, ZnCl**3**, H_2**2**, H_4**6** (CH_2Cl_2 solvate), and Ni**7** are summarized in Table 1, while data for H_4**6** (toluene solvate), Zn**2**, Ni**2**, and Pt**2** are provided in Supporting Information. The following software was used for crystallographic analysis: COLLECT[30] for data collection; DENZO and SCALEPACK[31] for cell refinement and data reduction; SIR92[32] and SIR97[33] for structure solution; and CRYSTALS[34] for refinement. All structures were refined on *F*.

Acknowledgment. We thank DSTL (Defense Science and Technology Laboratory, DSTL, Malvern) for financial support, Swansea Mass Spectrometry Service Centre for FAB mass spectra, and Dr. K. J. McEwan (DSTL, Malvern) for recording the near-infrared absorption spectra of the hexaphyrin in Figure 8.

Supporting Information Available: Synthetic procedures and spectroscopic data for ZnCl**3**, Zn**2**, Ni**2**, Pt**2**, and Ni**7**; crystallographic data for H_4**6** (toluene solvate), Zn**2**, Ni**2**, and Pt**2**; and X-ray crystallographic files for H**3**, ZnCl**3**, H_2**2**, Zn**2**, Ni**2**, Pt**2**, H_4**6** (CH_2Cl_2 solvate), H_4**6** (toluene solvate), and Ni**7** (CIF). This material is available free of charge via the Internet at http://pubs.acs.org.

JO026748C

(30) Nonius, B. V. *COLLECT*; Nonius: Delft, The Netherlands, 1997−2001.

(31) Otwinowski, Z.; Minor, W. In *Methods in Enzymology*, *Macromolecular Crystallography*; Carter, C. W., Sweet, R. M., Eds.; London: Academic Press, 1997; Vol. 276, Part A, pp 307−326.

(32) Altomare, A.; Cascarano, G.; Giacovazzo, C.; Guagliardi, A.; Burla, M. C.; Polidori, G.; Camalli, M. *J. Appl. Crystallogr.* **1994**, *27*, 435.

(33) Altomare, A.; Burla, M. C.; Camalli, M.; Cascarano, G.; Giacovazzo, C.; Guagliardi, A.; Moliterni, A. G. G.; Polidori, G.; Spagna, R. *J. Appl. Crystallogr.* **1999**, *32*, 115−118.

(34) Watkin, D. J.; Prout, C. K.; Carruthers, J. R.; Betteridge, P. W.; Cooper R. I. *CRYSTALS*, *Issue 11*; Chemical Crystallography Laboratory: Oxford, England, 2001.